Available online at www.sciencedirect.com

SciVerse ScienceDirect

Advances in Space Research 51 (2013) 2145–2154

ADVANCES IN SPACE RESEARCH (a COSPAR publication)

www.elsevier.com/locate/asr

Numerical modeling of inhomogeneous orographic wave influence on planetary waves in the middle atmosphere

Nikolai M. Gavrilov [a,*], Andrej V. Koval [a], Alexander I. Pogoreltsev [b], Elena N. Savenkova [b]

[a] Atmospheric Physics Department, Saint-Petersburg State University, Saint-Petersburg 198504, Russia
[b] Meteorological Forecast Department, Russian State Hydro-Meteorological University, Saint-Petersburg, Russia

Received 7 July 2012; received in revised form 24 December 2012; accepted 27 December 2012
Available online 8 February 2013

Abstract

Parameterization of dynamical and thermal effects of stationary orographic gravity waves (OGWs) generated by the Earth's surface topography is incorporated into a numerical model of general circulation of the middle and upper atmosphere. Responses of atmospheric general circulation and characteristics of planetary waves at altitudes from the troposphere up to the thermosphere to the effects of OGWs propagating from the earth surface are studied. Changes in atmospheric circulation and amplitudes of planetary waves due to variations of OGW generation and propagation in different seasons are considered. It is shown that during solstices the main OGW dynamical and heat effects occur in the middle atmosphere of winter hemispheres, where changes in planetary wave amplitudes due to OGWs may reach up to 50%. During equinoxes OGW effects are distributed more homogeneously between northern and southern hemispheres.

Keywords: Middle and upper atmosphere; Circulation; Modeling; Planetary waves; Orographic waves; Mountain waves

1. Introduction

Energy and momentum transport by internal atmospheric waves is currently considered to be an important factor of dynamical coupling between lower and upper atmosphere and a substantial contributor to space weather developments (Kelley, 1997). Numerical modeling of the general circulation and thermal regime of the middle and upper atmosphere increases attention to the study of accelerations of the mean flow and heating rates produced by dissipating internal waves in the atmosphere. One of the major sources of such waves is the Earth surface topography (Gossard and Hooke, 1975). Orographic waves generated as the result of interaction between height inhomogeneous surface and incoming mean flow may propagate into the middle atmosphere and produce substantial accelerations of the mean flow and heating rates, which may influence the general circulation, the thermal regime and the characteristics of planetary waves there (Holton, 1975; Fritts and Alexander, 2003). Simplified algorithms to parameterize thermal and dynamical effects of orographic waves have been developed, for example, by Young-Joon and Arakawa (1995), Lott and Miller (1997), Scinocca and McFarlane (2000), Vosper and Brown (2007), Catry et al. (2008), Geller et al. (2011). When calculating vertical profiles of wave accelerations of the mean flow and heating rates, it is essential to take into account the atmosphere rotation, which may substantially influence characteristics of stationary orographic gravity waves (OGW) with ground-based observed frequencies $\sigma = 0$ (see Section 2 below).

It is known that the surface topography and jet streams in the troposphere have inhomogeneous distributions over the globe, and wave sources and wave filtering in the atmosphere are subject to seasonal variations (Gavrilov and

* Corresponding author. Address: Atmospheric Physics Department, Saint-Petersburg State University, 1 Ul'yanivskaya Street, Petergof, Saint Petersburg 198504, Russia. Tel.: +7 812 4284489; fax: +7 812 4287240.
E-mail address: gavrilov@pobox.spbu.ru (N.M. Gavrilov).

0273-1177/$36.00 © 2013 COSPAR. Published by Elsevier Ltd. All rights reserved.
http://dx.doi.org/10.1016/j.asr.2012.12.024

Fukao, 1999) leading to differences of wave characteristics between winter and summer hemispheres. Satellite measurements of mesoscale variability of radiance, temperature and refraction coefficient in the atmosphere revealed substantial inhomogeneity of latitude-longitude distributions of orographic wave characteristics in the tropo-stratosphere, which significantly depend on season (Eckermann and Preusse, 1999; Preusse et al., 2002; Jiang et al., 2002; Smith et al., 2009; Gavrilov, 2007). This makes it essential to account for observable inhomogeneity of the wave source distributions in numerical models of general circulation of the middle atmosphere.

There were a number of numerical studies of gravity wave influence on the amplitudes and seasonal variations of tides (McLandress, 2002; Ortland and Alexander, 2006; Watanabe and Miyahara, 2009). Inhomogeneity of gravity wave sources and propagation conditions in the middle atmosphere may lead to the generation of planetary waves with variable characteristics (Holton, 1984; Mayr et al., 2011; Hoffmann et al., 2012).

In this paper, a parameterization of dynamical and thermal effects of OGWs generated by the Earth's surface topography (Koval and Gavrilov, 2011; Gavrilov and Koval, 2013) is incorporated into a numerical model of general circulation of the middle and upper atmosphere. The responses of general circulation of the atmosphere at altitudes from the troposphere up to the thermosphere to the effects of OGWs propagating from the troposphere are studied. Changes in amplitudes of stationary and propagating planetary waves due to OGW influence are estimated.

2. Parameterization of OGW effects

An important source of mesoscale stationary waves in the atmosphere can be atmospheric flow over mountains and other surface obstacles. Gavrilov and Koval (2013) described a new parameterization for dynamical and thermal effects caused by stationary OGWs, which is used in this study. To calculate vertical profiles of total vertical wave energy flux and amplitude of horizontal velocity we use polarization relations for stationary orographic waves taking account of the atmosphere rotation.

According to the theory of stationary mesoscale perturbations generated by air flowing over mountains, these disturbances may be attributed to internal gravity waves with ground-based observed frequencies $\sigma = 0$. Propagation of such waves in heterogeneous atmosphere with dissipation leads to an energy exchange between the background flow and waves, and to heating of the atmosphere due to wave energy dissipation. According to Gavrilov (1990), the equation of wave energy balance in the case of stationary and horizontally homogeneous atmosphere has the following form:

$$\frac{\partial F_E}{\partial z} = -\bar{\rho} D - \bar{\rho}\bar{v}_\alpha a_{w\alpha}, \quad a_{w\alpha} = -\frac{1}{\bar{\rho}}\frac{\partial(\bar{\rho}\overline{v'_\alpha w'})}{\partial z}, \qquad F_E = \overline{p'w'} + \bar{\rho}\bar{v}_\alpha\overline{v'_\alpha w'} - \overline{(\sigma'_{z\beta} + \tau'_{z\beta}x)v'_\beta} \tag{1}$$

where p and ρ are atmospheric pressure and density, respectively; v_α and w are velocity components along horizontal axes x_α and vertical axis z, respectively; repeating Greek indices denote summation; F_E is the total wave energy flux summarizing wave energy propagation and its transfer by background flow and turbulent and molecular diffusion; D is the wave energy dissipation rate; $a_{w\alpha}$ are components of wave acceleration of the mean flow involved in the hydrodynamic equations for horizontal components of the mean velocity; $\sigma_{\alpha\beta}$ and $\tau_{\sigma\beta}$ are tensors of molecular and turbulent viscous stresses, respectively; upper horizontal overlines denote averaging over the wave period and primes denote wave components of respective values.

On the right side of the first equation in (1), there are terms that describe the rate of wave energy dissipation and the work of forces arising due to nonlinear interaction between the wave and the mean flow, which depends on the mean flow velocity and wave acceleration. To describe correctly the energy balance of the considered dynamical processes, it is important to know the ratio between these sources and sinks of the wave energy. Gavrilov (1990) showed that in the presence of vertical gradient of the mean wind one can derive analytical relations between the rate of wave energy dissipation and the wave acceleration. These relations are used in the present study.

Gavrilov (1990) obtained approximate analytical expressions for F_E and for total heating rate ε_w produced by mesoscale stationary waves. The disadvantage of these formulae is that they give zero values for F_E and ε_w in case of stationary gravity waves having $\sigma = 0$. To obtain more correct expressions for F_E and ε_w, Gavrilov and Koval (2013) took into account the atmosphere rotation. Standard theory of atmospheric waves in flat rotating atmosphere (see, for example, Gossard and Hooke, 1975) gives polarization relations, which can be simplified for stationary gravity waves with frequency $\sigma = 0$ and large enough vertical $|m| \gg 1/(2H)$ and horizontal $k^2 \gg (f/c)^2$ wave numbers (where H is the atmospheric scale height, c is the speed of sound, f is the Coriolis parameter). Analysis of these polarization relations (see Gavrilov and Koval, 2013) shows that amplitude U of velocity variations v_k along the axis x_k parallel to the horizontal wave vector $\boldsymbol{k}$ is much larger than amplitude V of velocity fluctuations in the perpendicular direction. In this case, using relations by Gavrilov (1990) and Gavrilov and Koval (2013) one can get the following expressions for total wave energy flux, wave acceleration along axis x_k, and for total heating rate ε_w produced by mesoscale stationary waves:

$$F_E = -\frac{\bar{\rho} f^2 U^2}{2mk\bar{v}_k}; \quad m^2 = \frac{N^2}{\bar{v}_k^2}\left(1 - \frac{f^2}{k^2\bar{v}_k^2}\right)^{-1}. \qquad a_{wk} = -\frac{m^2U^2}{2\bar{v}_k}(\nu + K_z)\left(1 + \frac{1}{(\gamma-1)\mathrm{Pr}}\right), \qquad \varepsilon_w = (\nu + K_z)\delta m^2 U^2, \tag{2}$$

where ν and K_z are kinematic coefficients of molecular and turbulent viscosity, respectively; N is Brunt–Vaisala frequency; Pr is effective Prandl number equal to the ratio

of the sums of coefficients of molecular and turbulent viscosity and thermal conductivity; δ is a factor depending on vertical gradients of the mean wind (see Gavrilov and Koval, 2013). When $\delta = 1$, the expression for ε_w in (2) coincides with the expression for the rate of wave energy dissipation due to molecular and turbulent viscosity, which is often used to estimate thermal effects of stationary mesoscale waves. From (1) and the first relation in (2) one can get the approximate equation that describes the change of U^2 with height and, accounting for the major term on the right side, has the form of

$$\frac{\partial}{\partial z}\left(\frac{\bar{\rho} f^2 U^2}{2|k|N}\sqrt{1-\frac{f^2}{k^2\bar{v}_k^2}}\right) = -\bar{\rho}(v + K_z)\delta m^2 U^2. \quad (3)$$

Given the wave amplitude at the bottom boundary, the equation (3) can be solved for U^2 for specified vertical profiles of background wind and temperature. Then relations (2) allow us to calculate wave acceleration and total heating rate produced by OGW, which can be used to take into account dynamical and heating effects of stationary mesoscale orographic waves in atmospheric dynamic models.

To parameterize mesoscale topography in this work we use a modification of the method developed by Scinocca and McFarlane (2000). This method uses the concept of "subgrid orography", which takes account of the Earth's surface height variations with horizontal dimensions smaller than the horizontal grid step of the used numerical model. Our parameterization selects the subgrid topography using low- and high-frequency numerical filtering of realistic horizontal distributions of the Earth's surface elevations. These filters use averaging over parts of the surface with Gauss weight functions. Characteristics of the filters are chosen to effectively select variations of the Earth's surface elevations in the range of horizontal scales from about 20 km to the step length of the horizontal grid of the circulation model (5–6° in latitude and longitude – see Section 3), which is recommended by Scinocca and McFarlane (2000). In the vicinity of each point of the horizontal grid, according to Lott and Miller (1997), we use an elliptical approximation of the subgrid-scale relief. The analysis of forces acting on an atmospheric flow moving towards the effective elliptic mountain barrier made by Phillips (1984) allows us to determine OGW amplitude and effective horizontal wave number at the low boundary, which are necessary for the above calculation of vertical profiles of wave acceleration and heat influxes (see Gavrilov and Koval, 2013). For practical implementation of OGW parameterization described in this section we use the ETOPO2 (2012) database of the Earth's surface elevations with resolution of 2 min along latitude and longitude.

3. Numerical model of the general circulation of the atmosphere

For examining the OGW impact on the atmospheric dynamics, the parameterization described above was included into the middle and upper atmosphere model (MUAM) of atmospheric general circulation (Pogoreltsev, 2007; Pogoreltsev et al., 2007), which was developed on the basis of the COMMA-LIM model (Cologne Model of the Middle Atmosphere – Leipzig Institute for Meteorology, Froehlich et al., 2003). The basis for these modifications is the model COMMA developed earlier in Cologne University, Germany (Jakobs et al., 1986). A brief description of its main equations and physical processes taken into account was given by Gavrilov et al. (2005). The model is based on the standard system of primitive equations in spherical coordinates. It takes into account the processes of radiative heating and cooling of the atmosphere by gas components of O, O_2, O_3, H_2O, CO_2, and NO. The model uses parameterizations of atmospheric heating in ultraviolet and visible spectral ranges at wavelengths from 125 to 700 nm, and cooling due to 8; 9.6; 14 and 15 μm bands of infrared radiation. At altitudes of lower thermosphere, additional sources of heating due to dynamical processes are taken into account including ion drag, molecular viscosity and heat conduction as well as turbulent diffusion. The model provides the possibility of planetary wave generation near the Earth's surface. One can also change albedo of the underlying surface.

Calculations are carried out for heights from the ground up to the lower thermosphere, but the weather changes and cloudiness in the troposphere are not modeled. The set of model parameters includes zonal, meridional, and vertical components of velocity, geopotential, and temperature. A splitting procedure by Marchuk (1974) and Strang (1968) and the scheme proposed by Matsuno (1966) for time integration are used in the MUAM. To maintain solution stability, a Fourier transform filter is applied, which restricts horizontal resolution to ~500 km. The horizontal grid steps are 5.6° in longitude and 5° in latitude ranges from 87.5° S up to 87.5° N. Vertical grid of the model has a constant step in coordinate $z = \mathrm{H}\ ln\ (p_0/p)$, where p_0 is surface pressure and $H = 7$ km. Different versions of MUAM have 48 or 64 vertical grid points with step Δz of about 2.7 km. In present calculations we use the model version having 48 height levels and the integration time step of 450 s.

As lower boundary conditions at isobaric level of 1000 HPA, the zonal mean climatological distributions of geopotential height and temperature are specified. In predictive equation for temperature an additional term proportional to the difference between the calculated and observed zonal mean temperature in the troposphere and lower stratosphere is added, using the UK Met Office Model (Swinbank and O'Neill, 1994). The factor of proportionality is a reversed characteristic time scale of relaxation of calculated temperature to the observed one. The latter is set to 5 days. This allows us to realistically reproduce locations and intensity of tropospheric jet streams in the numerical experiments, which is necessary for correct simulation of propagation of stationary planetary and orographic waves from the troposphere into the stratosphere.

As OGW amplitudes are small in the boundary layer, calculation of vertical profiles of wave accelerations and heat influxes using the parameterization described in Section 2 starts from altitude of 7 km to which OGW surface characteristics are extrapolated. Calculated vertical profiles of wave heat influxes, zonal and meridional components of wave accelerations are added to the equations of heat balance and to the equations for respective velocity components of MUAM.

To specify initial distributions of hydrodynamic fields for the numerical modeling, a windless model of stratified atmosphere with realistic vertical temperature profile is used. During the first 150 days of model calculations, several stages of "adjustment" are performed. During the first 30 model days, the calculations are conducted for a constant value of geopotential height on the bottom boundary, and its observed changes are taken into account starting from the 31-st day of calculations. During the first 120 days, the calculations are performed accounting only for the daily average heating rates of the atmosphere, then daily variations of heating are gradually included and an additional predictive equation for the geopotential at bottom boundary is used. The calculations up to the 150th in-model day are performed for a fixed position of the Earth in orbit, and then the model takes into account seasonal changes of solar heating. Starting dates for calculations in different seasons are adjusted so that 151–210 in-model days would correspond to January–February, April–May, July–August and October–November.

4. Results of calculations

To study the influence of orographic waves generated by the Earth's surface relief and propagating upwards on the general circulation and the thermal regime of the middle atmosphere, calculations were performed using the described model MUAM involving OGW dynamic and thermal effects (see Section 2). Calculations were conducted for conditions corresponding to different seasons. For each set of initial data, hydrodynamic fields (wind speed, temperature, geopotential, etc.) were calculated including and excluding parameterization of OGW impacts. Differences in the hydrodynamic variables between these calculations show the velocity increment (VI), temperature increment (TI) or geopotential increment (GI) caused by OGW dynamic and thermal effects in the middle atmosphere. Positive or negative values of VI, TI and GI mean an increase or decrease in hydrodynamic variables caused by accounting for OGW effects.

4.1. Zonal mean distributions

Fig. 1(a) shows zonal wind averaged over longitude for January at heights from the surface to 140 km, calculated with the MUAM model. One can see that the model reasonably well reproduces basic features of zonal jet streams in the middle atmosphere. In the troposphere of the northern (winter) and the southern (summer) hemispheres, Fig. 1(a) reveals jet streams directed from West to East, with a maximum speed of about 30 m/s at the latitudes of 30–50° in both hemispheres. In winter in the stratosphere of the northern hemisphere, zonal flow does not change the direction and the jet stream velocity increases up to a maximum at altitude about 60 km and latitudes 50–60° S. In summer strato-mesosphere (southern hemisphere in Fig. 1(a)), zonal wind direction is from East to West with maximum speed at altitudes 50–70 km.

At heights of 90–120 km in Fig. 1(a), the general circulation in both hemispheres reverses and is directed from West to East in the winter (northern) hemisphere and from East to West in the summer (southern) hemisphere. Mentioned features of the middle atmosphere circulation are known and associated with peculiarities of altitude–latitude distributions of heat influxes in the middle atmosphere in different seasons (Holton, 1975). The structure of zonal circulation presented in Fig. 1(a) and respective temperature fields calculated with the MUAM correspond quite well to the existing empirical standard models (Jacobi et al., 2009; Pogoreltsev et al., 2009).

The inhomogeneity of the zonal circulation shown in Fig. 1(a) affects propagation of orographic waves. This can be seen in Fig. 1(b), which shows the zonal mean OGW amplitude for January. In the summer strato-mesosphere of the southern hemisphere, in regions, where the wind velocity tends to zero, the vertical wavelengths of stationary waves also tend to zero. This in turn causes low saturation amplitudes and strong wave dissipation. Accordingly, wind reversals produce critical levels and cause effective barriers for upward propagating OGWs, therefore wave amplitudes decrease above 20 km in the middle and high latitudes of summer (southern) hemisphere in Fig. 1(b). At low latitudes of the summer (southern) hemisphere and in the winter (northern) hemisphere, OGW amplitudes have significant values up to greater heights in Fig. 1(b). Gavrilov and Koval (2013) illustrated that the vertical profiles of OGW amplitudes may depend on profiles of average wind, temperature, molecular and turbulent viscosity and thermal conductivity. At low dissipation rates in the lower atmosphere, OGW amplitudes may grow quasi-exponentially with height. At higher altitudes increased kinematic molecular and turbulent viscosity and heat conductivity can lead to a weakening of OGWs with small vertical lengths. This may explain larger OGW amplitudes in winter (northern) hemisphere up to altitudes of 80–90 km seen in Fig. 1(b). Similar results on the predominance of OGW amplitudes in the middle atmosphere of the winter hemisphere have been obtained with a numerical simulation by Scinocca and Sutherland (2010). Increases in amplitudes of mesoscale waves in the strato-mesosphere of winter hemisphere were observed in many experiments (see, for example, seasonal changes in amplitudes of mesoscale waves at altitudes 20–40 km according to infrared sensing devices SABER and AIRS from the

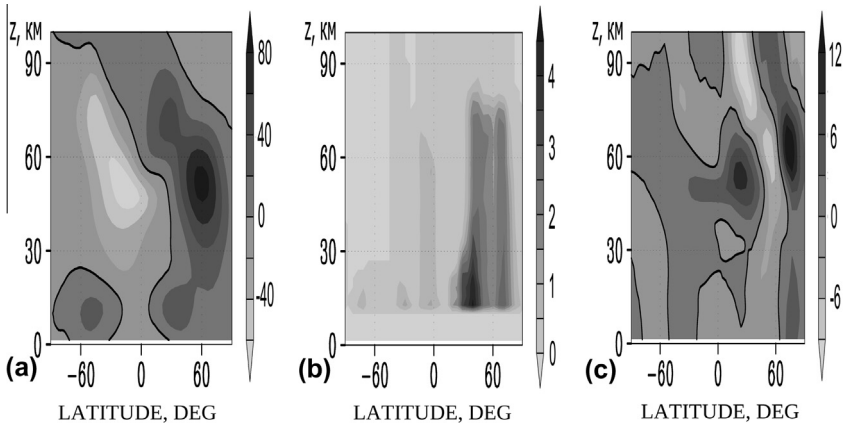

Fig. 1. Calculated with the MUAM zonal mean values of (a) zonal wind (m/s); (b) amplitude of OGW velocity variations in m/s; (c) increments in zonal circulation velocity (VI) in m/s due to OGW impacts for January. Solid contours show zero values.

boards of TIMED and Aqua satellites, respectively (Preusse et al., 2009; Gong et al., 2012), as well as from an analysis of measurements with GPS satellite CHAMP (Gavrilov, 2007)).

Calculations of zonal-mean altitude-latitude structure of OGW amplitudes for the other seasons have shown that in July, compared with the Fig. 1(b), northern and southern hemispheres change places. In the strato-mesosphere of northern (now summer) hemisphere a westward flow is developed, which leads to OGW filtering at critical levels. In the winter (southern) hemisphere in July OGW can propagate to greater heights, with OGW amplitudes here being on average smaller than those in the northern hemisphere in January because of the larger amount of mountain systems in the northern hemisphere (see Gavrilov and Koval, 2013). In spring and autumn, changes in circulation occur in the strato-mesosphere, when westward flows are destroyed and influence OGW filtering less. Therefore, OGW amplitudes in the middle atmosphere during equinoxes are more homogeneously distributed between the southern and northern hemispheres and OGW maximum in April are by 10–20% less than that in October.

Fig. 1(c) presents altitude-latitude structure of the zonal mean wind velocity differences in January, obtained as a difference between the velocity of circulation, calculated including and excluding parameterization of OGW effects in the numerical model (see above). One can see that the greatest changes in circulation velocity occur in winter (northern) hemisphere, where larger OGW amplitudes exist in Fig. 1(b). At altitudes 60–120 km in southern hemisphere one can see alternating areas of positive (up to 20 m/s) and negative (up to −15 m/s) VI values in Fig. 1(c). In these areas, respectively, strengthening and weakening of the eastward circulation velocity in the middle atmosphere occur due to OGW effects. In the middle atmosphere of summer (southern) hemisphere in January, positive VIs are detected at low and middle latitudes in Fig. 1(c).

Similar calculations for July confirm larger OGW influence on zonal circulation in winter (now southern) hemisphere. Basically, at altitudes 30–70 km in the southern hemisphere in winter alternating areas of positive VI (up to 15 m/s) and negative VI (up to −12 m/s) are available. Also in winter (southern) hemisphere at altitudes 70–120 km, areas of negative and positive VI exist. OGW effects on general circulation were calculated for equinoxes. In April at altitudes around 70 km, a slowing down of zonal circulation at 60–70° S, and an increase in its speed at 50–60° S were obtained, as well as changes in zonal circulation velocity at low latitudes of the northern hemisphere. In October, the changes in the zonal mean circulation up to 10% occur mainly in the mid-latitudes of the northern hemisphere.

4.2. OGW influence on planetary waves

Gavrilov et al. (2013) studied latitude-longitude distributions of hydrodynamic variables, at fixed altitudes. The results of numerical simulations described above show that in addition to the wave oscillation OGW may create disturbances of wind and temperature over large areas, which are caused by changes in circulation due to the impact of wave accelerations and heat influxes. Therefore, perturbations of atmospheric parameters related to OGWs may span large territories and may occur not only over the mountain systems themselves, but also at a considerable distance from the mountains. Heterogeneous distribution of mountain ranges and tropospheric flows around the globe and associated heterogeneity of characteristics of generated OGWs may lead to significant changes in the general circulation of the middle and upper atmosphere.

Changing winds in the troposphere during the simulation in consecutive days lead to displacements of VI maxima and minima both in West and East directions. OGW propagation is also affected by the mean wind and temperature distributions in the entire atmosphere column, which may change during the experiment. Therefore, numerical

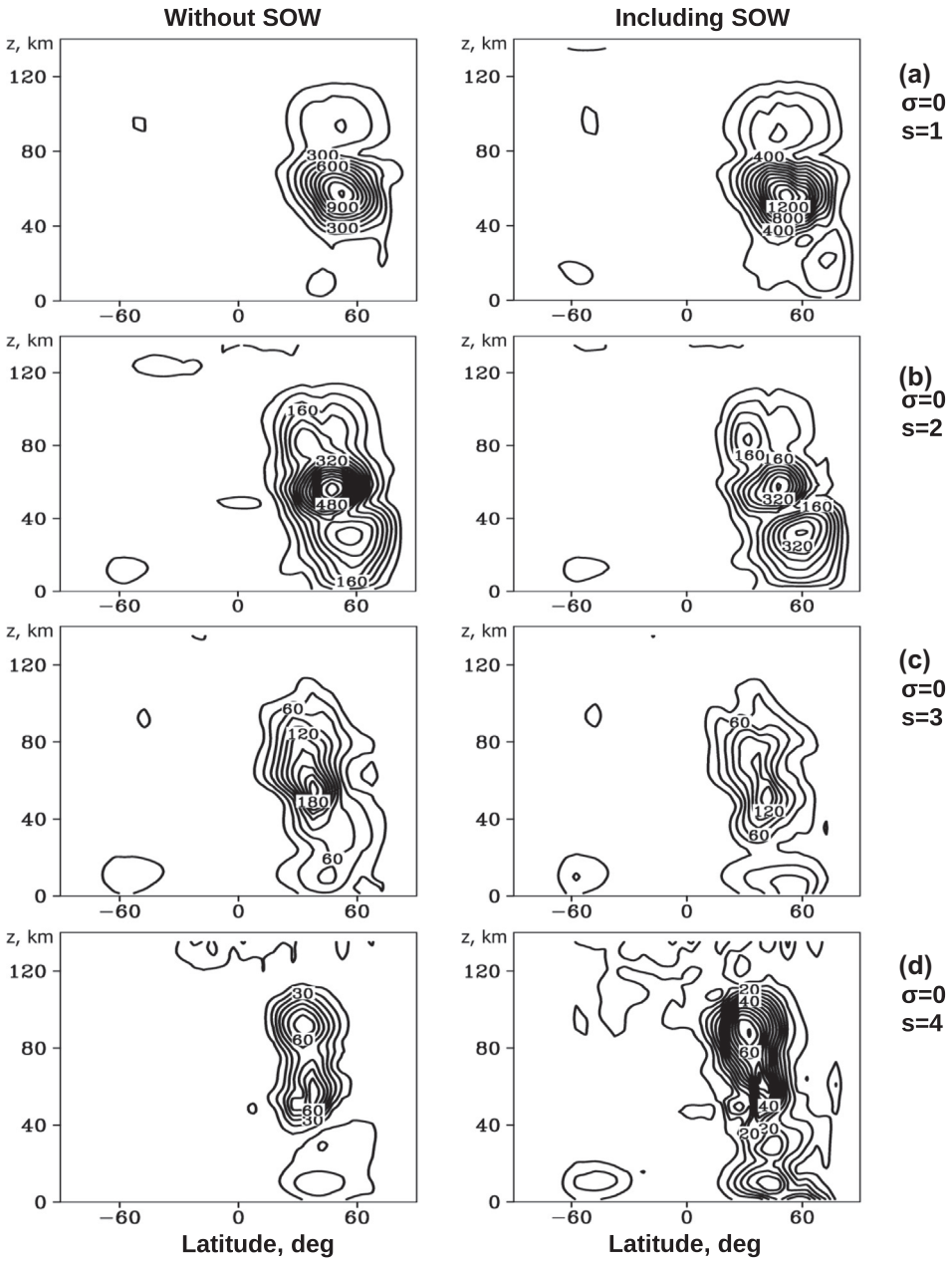

Fig. 2. Amplitudes of geopotential height variations (in gpm) produced by stationary planetary waves having different zonal wave numbers s and calculated for January without (left) and including (right) parameterization of OGW dynamical and thermal effects.

experiments show permanent displacements of VI extremes, similar to propagation of planetary scale waves.

To analyze OGW influence on parameters of planetary waves, we decompose meteorological fields calculated by the MUAM into components having frequencies $\sigma = 2\pi/\tau$ (τ being wave period) and zonal wave numbers $s = 0$–4. Using the information about the amplitudes and phases of these harmonics calculated using the least squares fit to longitudes, we can separate the wave fields into the eastward and westward propagating modes as it was suggested by Fedulina et al. (2004). We made calculations for a wide set of τ and s values. In this paper we present some cases, when OGW effects produce substantial changes in amplitudes of planetary wave modes in the middle atmosphere.

Fig. 2 shows amplitudes of geopotential height variations caused by stationary planetary waves having $\sigma = 0$ and different zonal wave numbers s. These waves are generated in the MUAM by specifying appropriate distributions of geopotential height and temperature perturbations at the lower boundary (1000 h Pa). Left and right plots in Fig. 2 correspond to calculations without accounting for OGWs and including the parameterization of OGW dynamical and thermal effects in the numerical model. Fig. 2 shows that in January stationary planetary waves propagate mainly in winter (northern) hemisphere. Comparison of left and right plots of Fig. 2 shows that OGW influence above altitude 40 km leads to an increase in amplitudes of the planetary wave modes $s = 1$ and

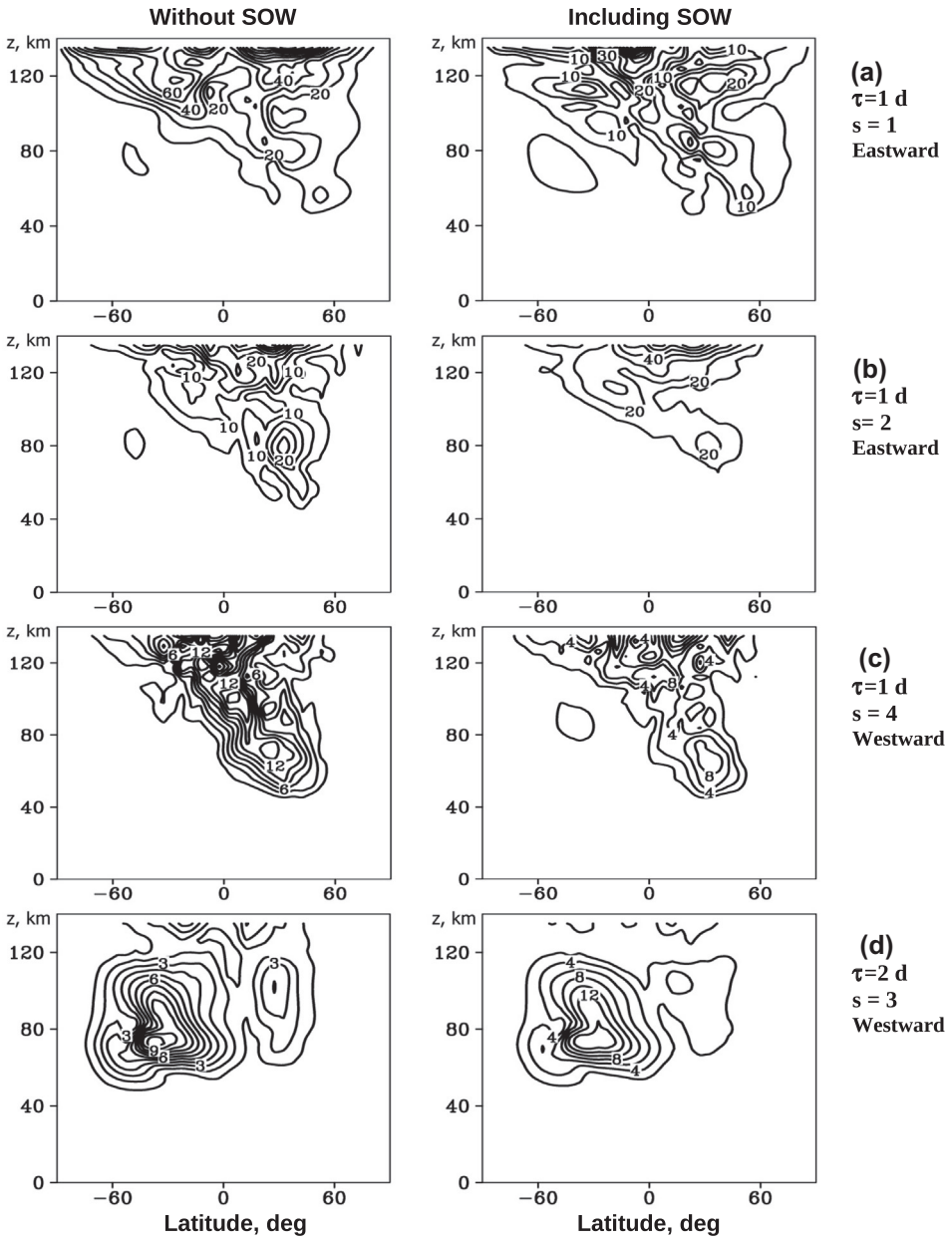

Fig. 3. Examples of amplitudes of geopotential height variations (in gpm) produced by planetary waves having different periods τ (in days) and zonal wave numbers s, and propagating westwards or eastwards, which are calculated for January without (left) and including (right) parameterization of OGW dynamical and thermal effects.

$s = 4$ and to a decrease in amplitudes of the modes $s = 2$ and $s = 3$. For almost all waves in Fig. 2 amplitudes increase below altitude 40 km due to OGW influence. In the right plot of Fig. 2(c), accounting for OGW effects, amplitudes of the wave mode $s = 3$ are smaller than that in the left plots at all altitudes.

Besides stationary planetary waves, their propagating modes exist in the atmosphere. In our modeling we did not specify special sources of propagating planetary waves. Therefore, they may be produced in the model runs due to global-scale inhomogeneities of radiation heat sources in the model, due to nonlinear interactions between non-stationary general circulation and stationary planetary waves, and due to inhomogeneities of mesoscale OGW sources. Figs. 3 and 4 illustrate some examples, when taking account of parameterization of OGW dynamical and thermal effects in the model leads to substantial changes in amplitudes of propagating planetary waves. For planetary waves with period $\tau = 1$ day taking account of OGW effects leads to a decrease in amplitudes of the eastward propagating mode having $s = 1$ (Fig. 3(a)) and the westward propagating $s = 4$ mode (Fig. 3(c)), and also to an increase in amplitudes of the westward propagating mode $s = 2$ in Fig. 3(b).

For two-day planetary waves, OGW effects increase amplitudes of both the westward propagating mode

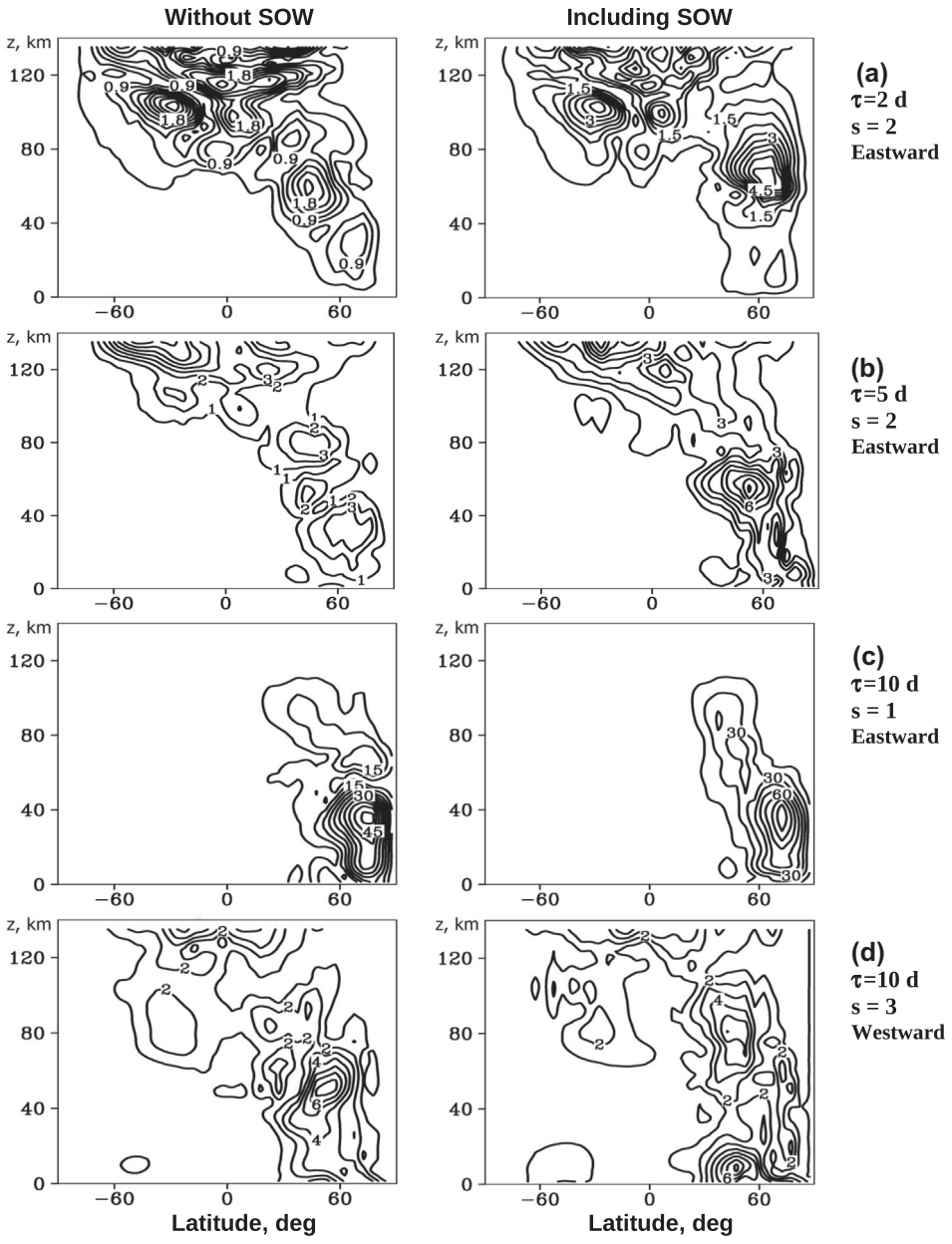

Fig. 4. Same as Fig. 3, but for different periods and zonal wave numbers of propagating planetary waves.

$s = 3$ (Fig. 2(d)) and the eastward propagating mode $s = 2$ in Fig. 3(a). Also one can see an increase in amplitude of the eastward propagating mode $s = 2$ of planetary waves with period $\tau = 5$ days at altitudes 50–70 km in the mid-latitudes of northern hemisphere in Fig. 4(b). For long-period planetary waves with $\tau = 10$ days, amplitudes with OGW effects are larger for the eastward propagating mode $s = 1$ in Fig. 4(c). But comparison of the left and right plots of Fig. 4(d) shows that for 10-day westward propagating planetary waves with $s = 3$ OGW effects increase amplitudes above altitude 60 km and below 20 km and decrease amplitudes at altitudes 20–60 km at mid-latitudes of northern hemisphere.

Consideration of Figs. 2–4 shows that in many cases taking account of OGW dynamical and thermal effects in the MUAM leads to an increase in amplitudes of stationary, eastward and westward propagating planetary waves. Sometimes, the amplitude increase may be up to 50%. Therefore, OGW generation by varying tropospheric flows over inhomogeneous mountain systems and wave propagation to the middle and upper atmosphere may produce changes in general circulation and amplitudes and other parameters of tides and planetary waves up to high altitudes as it was described in some previous publications (Holton, 1984; McLandress, 2002; Ortland and Alexander, 2006; Watanabe and Miyahara, 2009; Mayr et al., 2011; Hoffmann et al., 2012). Our analysis showed that changes

in amplitudes of the main modes of tides and planetary waves due to OGW effects are relatively small. But inhomogeneity of orographic wave sources and conditions of OGW propagation may lead to the generation of additional modes of planetary waves, some of which are shown in Figs. 2–4. Combined influence of accelerations of the mean flow and heat influxes produced by OGWs is rather complicated and may increase or decrease amplitudes of tides and planetary waves at different altitudes and geographic locations. Further studies of OGW influence tides and planetary waves are required.

5. Conclusion

In this paper, the authors include parameterization of dynamical and thermal effects of stationary orographic waves generated by the topography of the Earth's surface (Gavrilov and Koval, 2013) into a numerical model of the general circulation of the middle and upper atmosphere. Responses of general circulation and amplitudes of planetary waves in the atmosphere to influences of OGWs propagating from the troposphere are studied at altitudes from the troposphere to the thermosphere.

Calculated values of wave heat influxes up to 10 K/day and wave accelerations up to 20 ms^{-1}/day at altitudes around 50 km show that the orographic waves can produce a significant impact on the dynamic and thermal regimes of the middle and upper atmosphere. In January and July, the OGW influence may produce changes in zonal circulation velocity up to 20 m/s in winter seasons of the northern and southern hemispheres, respectively. In the Equinoxes, OGW effects are more homogeneously distributed over both hemispheres

Taking account of OGW dynamical and thermal effects in the MUAM leads to changes in amplitudes of stationary, eastward and westward propagating planetary waves. Sometimes, the amplitude changes may be up to 50%. Therefore, OGW generation by varying tropospheric flows over inhomogeneous mountain systems and wave propagation to the middle and upper atmosphere may produce changes in general circulation and amplitudes and other parameters of planetary waves up to high altitudes.

Acknowledgements

The work was supported by Russian Foundation for Basic Research, as well as by Federal Education Agency within the federal program "Scientific-Pedagogical Personnel of Innovative Russia" for years 2009–2013.

References

Catry, B., Geleyn, J.-F., Bouyssel, F., Cedilnik, J., Broo, R., Derková, M., Mladek, R. A new sub-grid scale lift formulation in a mountain drag parameterisation scheme. Meteorol. Zeitschrift. 17 (2), 193–208, 2008.

Eckermann, S.D., Preusse, P. Global measurements of stratospheric mountain waves from space. Science 286, 1534–1537, 1999.

ETOPO2. Global Gridded 2-minute Database, National geophysical data center, national oceanic and atmospheric administration, US Department of Commerce, <http://www.ngdc.noaa.gov/mgg/global/etopo2.html>. 2012.

Fedulina, I.N., Pogoreltsev, A.I., Vaughan, G. Seasonal, interannual and short-term variability of planetary waves in met office stratospheric assimilated fields. Quart. J. R. Met. Soc. 130, 2445–2458, 2004.

Fritts, D.C., Alexander, M.J. Gravity wave dynamics and effects in the middle atmosphere. Rev. Geophys. 41 (1), 1003, http://dx.doi.org/10.1029/2001RG000106, 2003.

Froehlich, K., Pogoreltsev, A., Jacobi, Ch. Numerical simulation of tides, Rossby and Kelvin waves with the COMMA-LIM model. Adv. Space Res. 32 (5), 863–868, 2003.

Gavrilov, N.M. Parameterization of accelerations and heat flux divergences produced by internal gravity waves in the middle atmosphere. J. Atmos. Terr. Phys. 52 (9), 707–713, 1990.

Gavrilov, N.M. Structure of the mesoscale variability of the troposphere and stratosphere found from radio refraction measurements via CHAMP satellite. Izvestia Atmos. Oceanic Phys. 43 (4), 451–460, 2007.

Gavrilov, N.M., Fukao, S. A comparison of seasonal variations of gravity wave intensity observed with the middle and upper atmosphere radar with a theoretical model. J. Atmos. Sci. 56, 3485–3494, 1999.

Gavrilov, N.M., Koval, A.V. Parameterization of mesoscale stationary orographic wave impact for usage in numerical models of atmospheric dynamics. Izvestia Atmos. Oceanic Phys. 49 (3). Accepted, 2013.

Gavrilov, N.M., Pogoreltsev, A.I., Jacobi, Ch. Numerical modeling of the effect of latitude-inhomogeneous gravity waves on the circulation of the middle atmosphere. Izvestia Atmos. Ocean Phys. 41 (1), 9–18, 2005.

Gavrilov, N. M., Koval A. V., Pogoreltsev A. I., Savenkova E. N. Numerical modeling response of general circulation of the middle atmosphere on spacial inhomogeneities of orographic waves. Izvestia. Atmos. Ocean Phys. 49, Accepted, 2013.

Geller, M.A., Zhou, T., Ruedy, R., et al. New gravity wave treatments for GISS climate models. J. Climate 24, 3989–4002, http://dx.doi.org/10.1175/2011JCLI4013.1, 2011.

Gong, J., Wu, D.L., Eckermann, S.D. Gravity wave variances and propagation derived from AIRS radiances. Atmos. Chem. Phys. 12 (4), 1701–1720, 2012.

Gossard, E.E., Hooke, W.H. Waves in the Atmosphere. Elsevier Sci. Publ. Co., Amsterdam, Oxford, New York, 1975.

Hoffmann, P., Jacobi, Ch., Borries, C. A possible planetary wave coupling between the stratosphere and ionosphere by gravity wave modulation. J. Atmos. Solar-Terr. Phys. 75–76, 71–80, http://dx.doi.org/10.1016/j.jastp. 2011.07.008, 2012.

Holton, J.R. The dynamic meteorology of the stratosphere and mesosphere. Meteorol. Monogr. 15 (37), 1–218, 1975.

Holton, J.R. The generation of mesospheric planetary waves by zonally asymmetric gravity wave breaking. J. Atmos. Sci. 41 (23), 3427–3430, 1984.

Jacobi, Ch., Fröhlich, K., Portnyagin, Y., et al. Semi-empirical model of middle atmosphere wind from the ground to the lower thermosphere. Adv. Space Res. 43, 239–246, 2009.

Jakobs, H.J., Bischof, M., Ebel, A., Speth, P. Simulation of gravity wave effects under solstice conditions using a 3-D circulation model of the middle atmosphere. J. Atmos. Terr. Phys. 48, 1203–1223, 1986.

Jiang, J.H., Wu, D.L., Eckermann, S.D. Upper atmosphere research satellite (UARS) observation of mountain waves over the Andes. J. Geophys. Res. 107 (D20), 8273, http://dx.doi.org/10.1029/2002JD002091, 2002.

Kelley, M.C. Aspects of Weather and Space Weather in the Earth's Upper Atmosphere: The Role of Internal Atmospheric Waves. International Science Lecture Series, National Academy Press, Washington, D.C., 6, 1–31, 1997.

Koval, A.V., Gavrilov, N.M. Parameterization of orographic wave influence the general circulation of the middle and upper atmosphere. RSGMU Sci. Notes 20, 85–89 (in Russian), 2011.

Lott, F., Miller, M.J. A new subgrid-scale orographic drag parametrization: its formulation and testing. Quart. J. R. Meteorol. Soc. 1997 (123), 101–127, 1997.

Marchuk, G.I. Numerical Methods in Weather Prediction. Academic Press, New York, 1974.

Matsuno, T. Numerical integration of the primitive equations by a simulated backward difference method. J. Meteorol. Soc. Jpn. 44, 76–84, 1966.

Mayr, H.G., Mengel, J.G., Chan, K.L., Huang, F.T. Middle atmosphere dynamics with gravity wave interactions in the numerical spectral model: tides and planetary waves. J. Atmos. Solar-Terr. Phys. 73, 711–730, 2011.

McLandress, C. The seasonal variation of the propagating diurnal tide in the mesosphere and lower thermosphere. Part I: The role of gravity waves and planetary waves. J. Atmos. Sci. 59, 893–906, 2002.

Ortland, D.A., Alexander, M.J. Gravity wave influence on the global structure of the diurnal tide in the mesosphere and lower thermosphere. J. Geophys. Res. 111, A10S10, http://dx.doi.org/10.1029/2005JA011467, 2006.

Phillips, D.S. Analytical surface pressure and drag for linear hydrostatic flow over three-dimensional elliptical mountains. J. Atmos. Sci. 41, 1073–1084, 1984.

Pogoreltsev, A.I. Generation of normal atmospheric modes by stratospheric vacillations. Izvestia Atmos. Ocean Phys. 43 (4), 423–435, 2007.

Pogoreltsev, A.I., Kanukhina, A.Yu., Suvorova, E.V., Savenkova, E.N. Variability of planetary waves as a signature of possible climatic changes. J. Atmos. Solar-Terr. Phys. 71, 1529–1539, http://dx.doi.org/10.1016/j.jastp. 2009.05.011, 2009.

Pogoreltsev, A.I., Vlasov, A.A., Froehlich, K., Jacobi, Ch. Planetary waves in coupling the lower and upper atmosphere. J. Atmos. Solar-Terr. Phys. 69, 2083–2101, http://dx.doi.org/10.1016/j.jastp. 2007.05.014, 2007.

Preusse, P., Dornbrack, A., Eckermann, S.D., Riese, M., Schaeler, B., Bacmeister, J.T., Broutman, D., Grossman, K.U. Space-based measurements of stratospheric mountain waves by CRISTA: 1. Sensitivity, analysis method, and a case study. J. Geophys. Res. 107 (D23), 8178, http://dx.doi.org/10.1029/2001JD000699, 2002.

Preusse, P., Eckermann, S.D., Ern, M., et al. Global ray tracing simulations of the SABER gravity wave climatology. J. Geophys. Res. 114, D08126, http://dx.doi.org/10.1029/2008JD011214, 2009.

Scinocca, J.F., McFarlane, N.A. The parameterization of drag induced by stratified flow over anisotrophic orography. Quart. J. R. Meteorol. Soc. 126 (568), 2353–2393, 2000.

Scinocca, J.F., Sutherland, B.R. Self-acceleration in the parameterization of orographic wave drag. J. Atmos. Sci. 67 (8), 2537–2546, 2010.

Smith, S., Baumgardner, J., Mendillo, M. Evidence of mesospheric gravity-waves generated by orographic forcing in the troposphere. Geophys. Res. Lett. 36, L08807, http://dx.doi.org/10.1029/2008GL036936, 2009.

Strang, G. On the construction and comparison of difference schemes. SIAM J. Numer. Anal. 5, 516–517, 1968.

Swinbank, R., O'Neill, A. Stratosphere-troposphere assimilation system. Mon. Weather Rev. 122, 686–702, 1994.

Vosper, S.B., Brown, A.R. The effect of small-scale hills on orographic drag. Quart. J. R. Meteorol. Soc. 2007 (133), 1345–1352, 2007.

Watanabe, S., Miyahara, S. Quantification of the gravity wave forcing of the migrating diurnal tide in a gravity wave–resolving general circulation model. J. Geophys. Res. 114, D07110, http://dx.doi.org/10.1029/2008JD011218, 2009.

Young-Joon, K., Arakawa, A. Improvement of orographic gravity wave parameterization using a mesoscale gravity wave model. J. Atmos. Sci. 52 (11), 1875–1902, 1995.